

# The bioenergetic and antioxidant status of neurons is controlled by continuous degradation of a key glycolytic enzyme by APC/C–Cdh1

Angel Herrero-Mendez<sup>1</sup>, Angeles Almeida<sup>1,2</sup>, Emilio Fernández<sup>1</sup>, Carolina Maestre<sup>1,2</sup>, Salvador Moncada<sup>3,4</sup> and Juan P. Bolaños<sup>1,4</sup>

**Neurons are known to have a lower glycolytic rate than astrocytes and when stressed they are unable to upregulate glycolysis<sup>1</sup> because of low Pfkfb3 (6-phosphofructo-2-kinase/fructose-2,6-bisphosphatase-3) activity<sup>2</sup>. This enzyme generates fructose-2,6-bisphosphate (F2,6P<sub>2</sub>)<sup>3</sup>, the most potent activator of 6-phosphofructo-1-kinase (Pfk1; ref. 4), a master regulator of glycolysis<sup>5</sup>. Here, we show that Pfkfb3 is absent from neurons in the brain cortex and that Pfkfb3 in neurons is constantly subject to proteasomal degradation by the action of the E3 ubiquitin ligase<sup>6</sup>, anaphase-promoting complex/cyclosome (APC/C)–Cdh1. By contrast, astrocytes have low APC/C–Cdh1 activity and therefore Pfkfb3 is present in these cells. Upregulation of Pfkfb3 by either inhibition of Cdh1 or overexpression of Pfkfb3 in neurons resulted in the activation of glycolysis. This, however, was accompanied by a marked decrease in the oxidation of glucose through the pentose phosphate pathway (a metabolic route involved in the regeneration of reduced glutathione<sup>7</sup>) resulting in oxidative stress and apoptotic death. Thus, by actively downregulating glycolysis by APC/C–Cdh1, neurons use glucose to maintain their antioxidant status at the expense of its utilization for bioenergetic purposes.**

Using reverse-transcriptase polymerase-chain reaction (RT–PCR) in RNA extracts from terminally differentiated rat cortical neurons and astrocytes, we established that *Pfkfb* mRNA is expressed in neurons and that isoform 3 (*Pfkfb3*) mRNA is the most abundant in both cell types (Supplementary Information, Fig. S1a). This was confirmed by northern blotting (Fig. 1a, upper panel). Having demonstrated by RT–PCR that K6 was the most abundant splice variant of *Pfkfb3* mRNA, we raised an antibody against its carboxy-terminal domain (Supplementary Information, Fig. S1b, c) and used it to assess the expression of Pfkfb3 protein in

neurons and astrocytes. Pfkfb3 was undetectable by western blotting in neurons, whereas it was present in astrocytes (Fig. 1a, lower panels; Supplementary Information, Fig. S1d, e). Immunohistochemistry in coronal sections of rat brain cortex showed that Pfkfb3 did not colocalize with the neuronal nuclear marker NeuN but it did colocalize with the astrocyte marker GFAP (Fig. 1b). Thus, although *Pfkfb3* mRNA is present in neurons, Pfkfb3 protein is absent, suggesting that the enzyme is downregulated post-transcriptionally in these cells.

Incubation of neurons with the proteasome inhibitors MG132 or lactacystine for 1 h resulted in accumulation of Pfkfb3 protein (Fig. 1c, upper panel). Furthermore, immunoprecipitation of Pfkfb3 in either MG132- or lactacystine-treated neurons, followed by western blotting using an anti-ubiquitin antibody, revealed an increase in Pfkfb3 ubiquitylation (Fig. 1c, lower panel). These results indicate that in neurons Pfkfb3 is degraded through the ubiquitin–proteosome pathway, which has been described in myogenic cells during differentiation<sup>8</sup>. We then investigated possible motifs targeting Pfkfb3 for ubiquitylation and found that Pfkfb3, but not the 1, 2 or 4 isomers, contains a KEN box at position 142 (Supplementary Information, Fig. S1f). A KEN box targets proteins for ubiquitylation by the APC/C<sup>9</sup>. Activation of APC/C requires the formation of a complex with Cdc20 or Cdh1 (ref. 10); however, Cdh1 is the only possible activator of APC/C in the terminally differentiated neurons used in this study<sup>11</sup>. Cdh1 was knocked down in neurons using short interfering RNA (siRNA) and Pfkfb3 protein was found to accumulate (Fig. 1d). Cdh1 protein abundance (Fig. 1d) and APC/C activity (Fig. 1e) were lower in astrocytes than in neurons, and overexpression of Cdh1 in astrocytes decreased Pfkfb3 protein (Fig. 1f). Transfection of neurons with wild-type Pfkfb3 or a mutant form in which the KEN box was altered to AAA by site-directed mutagenesis, followed by flow cytometry sorting (using green fluorescent protein (GFP)<sup>+</sup> labelling) revealed greater accumulation of the mutant Pfkfb3 form than of the wild-type (Fig. 1g). These results demonstrate that although Pfkfb3

<sup>1</sup>Departamento de Bioquímica y Biología Molecular, Universidad de Salamanca, Instituto de Neurociencias de Castilla y León, 37007 Salamanca, Spain. <sup>2</sup>Unidad de Investigación, Hospital Universitario de Salamanca, Instituto de Estudios de Ciencias de la Salud de Castilla y León, 37007 Salamanca, Spain. <sup>3</sup>Wolfson Institute for Biomedical Research, University College London, Gower Street, London WC1E 6BT, UK.

<sup>4</sup>Correspondence should be addressed either to J.P.B. or S.M. (e-mail: jbolanos@usal.es; s.moncada@ucl.ac.uk)

Received 12 December 2008; accepted 17 February 2009; published online 17 May 2009; DOI: 10.1038/ncb1881

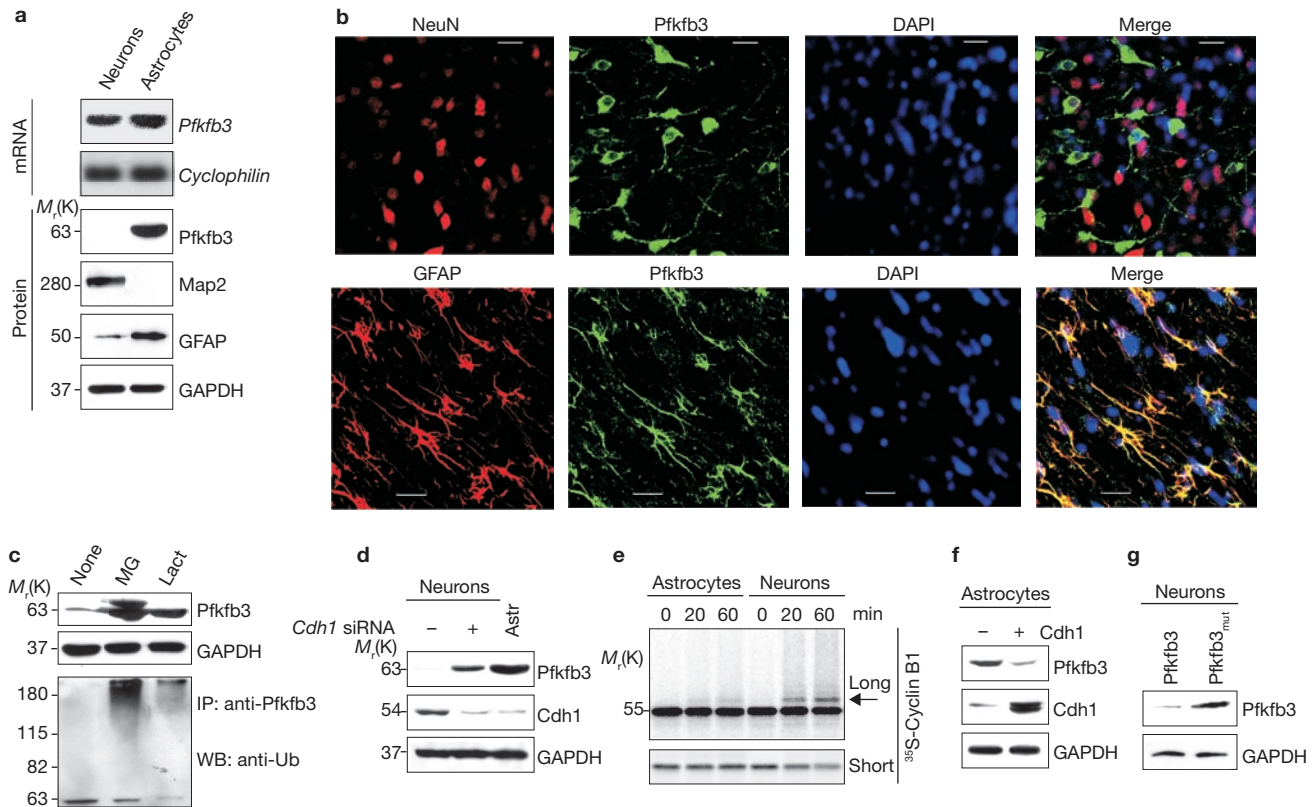


**Figure 1** Pfkfb3 protein is degraded through the ubiquitin–proteasome pathway mediated by APC/C–Cdh1 in rat cortical neurons but not in astrocytes. **(a)** Upper panel: northern blotting of total RNA extracts from terminally differentiated rat cortical neurons and astrocytes showed that similar amounts of *Pfkfb3* mRNA were expressed in each cell type. *Cyclophilin* was used as an mRNA loading marker. Lower panel: western blotting using an anti-Pfkfb3 antibody revealed the absence of Pfkfb3 protein expression in neurons, whereas Pfkfb3 was expressed abundantly in astrocytes. *Map2* was used as a neuronal marker, *GFAP* as a glial marker and *GAPDH* as a loading control. **(b)** Fluorescence microphotographs of coronal sections of rat brain cortex show immunohistochemically the absence of Pfkfb3 in neurons and its presence in astrocytes. Neurons and glial cells were identified using the specific markers *NeuN* and *GFAP*, respectively. Nuclei were identified using *DAPI*. Scale bars, 20  $\mu$ m. **(c)** Incubation of neurons with the proteasome inhibitors lactacystine or MG132 for 1 h resulted in

is subject to degradation by the action of APC/C–Cdh1 in neurons, Pfkfb3 protein is stable in astrocytes as a result of their low APC/C–Cdh1 activity. The results also indicate that post-transcriptional repression of Pfkfb1, 2 and 4 in neurons, if it occurs, is through a mechanism that is independent of APC/C–Cdh1.

We then investigated whether Cdh1 regulates glycolysis in neurons. Silencing Cdh1 increased both the glycolytic flux (Fig. 2a; Supplementary Information, Fig. S2a) and the concentration of intracellular lactate (Fig. 2b; Supplementary Information, Fig. S2b). These effects were abolished by co-silencing phosphoglucomutase (PGI), the glycolytic enzyme responsible for the formation of fructose-6-phosphate (F6P), which is the substrate of Pfk1 (Fig. 2a; Supplementary Information, Fig. S2c,d). The increase in the glycolytic flux induced by silencing Cdh1 was also abolished by co-silencing Pfkfb3 (Fig. 2a). Thus the low glycolytic rate in neurons can be accounted for by APC/C–Cdh1-mediated degradation of Pfkfb3.

Pfkfb3 accumulation, shown by western blotting. Immunoprecipitation of protein extracts with an anti-Pfkfb3 antibody, followed by western blotting against ubiquitin (Ub) showed increased Pfkfb3 protein ubiquitylation in the lactacystine- and MG132-treated neurons. **(d)** Silencing *Cdh1* in neurons at 3 days *in vitro* resulted in significant knockdown of Cdh1 protein and accumulation of Pfkfb3 (after 3 days) to approximately 50% of the level found in astrocytes, as assessed by densitometry; astrocytes express very little Cdh1 protein. **(e)** APC/C activity, measured as the ability to ubiquitylate <sup>35</sup>S-cyclin B1, is lower in astrocytes than in neurons (the arrow indicates the most abundant ubiquitylated form of cyclin B1; ‘long’ and ‘short’ indicate the exposure time of the film: short exposure allows visualization of the corresponding decrease in <sup>35</sup>S-cyclin B1). **(f)** Overexpression of Cdh1 in astrocytes decreases Pfkfb3 protein. **(g)** Wild-type Pfkfb3, but not a site-directed mutant form (<sup>142</sup>KEN to <sup>142</sup>AAA, Pfkfb3<sub>mut</sub>), is degraded when expressed in neurons using low amounts of cDNA.

Next we investigated whether an increase in the basal glycolytic rate would render neurons more resistant to stress. Glycolysis was increased initially by silencing Cdh1; however, this treatment enhanced neuronal apoptotic death, as assessed by flow cytometry of annexin V<sup>+</sup>/7-AAD<sup>-</sup> cells (Fig. 2c; Supplementary Information, Fig. S2e). The apoptosis caused by silencing Cdh1 was partially prevented by silencing PGI (Fig. 2c) or Pfkfb3 (Fig. 2d). Cyclin B1 also mediates, in part, apoptosis induced by silencing Cdh1 in neurons<sup>11</sup> (Fig. 2d), but co-silencing cyclin B1 and Pfkfb3 fully abolished apoptosis in *Cdh1* siRNA neurons (Fig. 2d). Thus, silencing Cdh1 in these cells triggers apoptosis through both cyclin B1 (ref. 11) and Pfkfb3. Neurons were then transfected with the full-length *Pfkfb3* cDNA and sorted by flow cytometry using GFP (Supplementary Information, Fig. S2f,g). This resulted in an increase in glycolytic flux (Fig. 2a) and an accumulation of lactate, which was prevented by silencing PGI (Fig. 2e). Expression of Pfkfb3 increased apoptosis in neurons in a concentration- (Fig. 2f) and time- (Fig. 2g) dependent

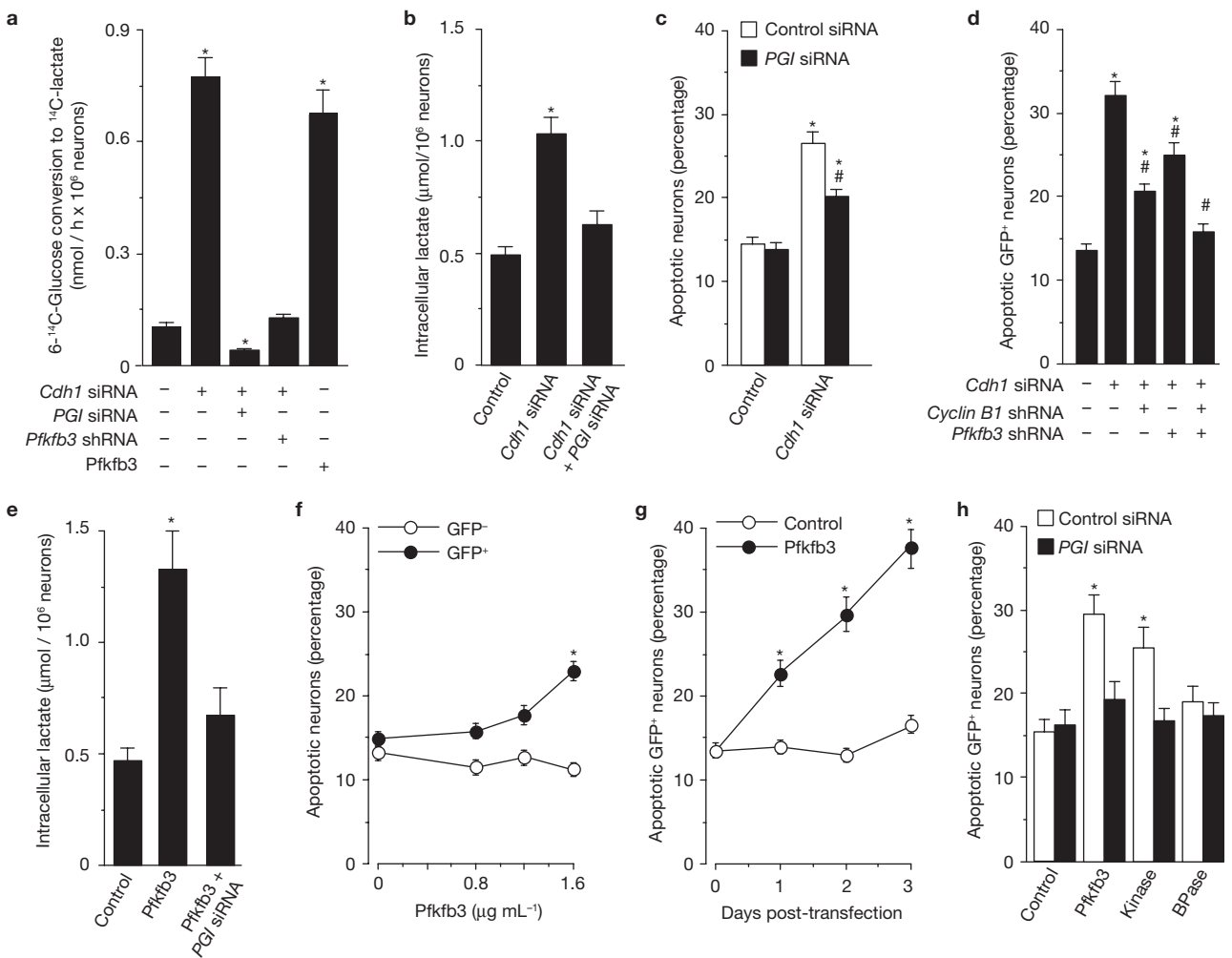


**Figure 2** Cdh1 downregulates glycolysis and protects against apoptotic death through Pfkfb3 degradation in neurons. **(a)** Transfection with *Cdh1* siRNA in neurons significantly increased the rate of glycolysis, measured as the rate of 6-<sup>14</sup>C-glucose conversion to <sup>14</sup>C-lactate; this effect was prevented by co-silencing *PGI* or *Pfkfb3*, and was mimicked by overexpression of Pfkfb3. Left histogram bar corresponds to control (luciferase) siRNA/shRNA. **(b)** Silencing *Cdh1* increased intracellular lactate concentrations, an effect that was prevented by co-silencing *PGI*. **(c)** *Cdh1* siRNA increased the proportion of apoptotic (annexin V<sup>+</sup>/7-AAD<sup>-</sup>) neurons, an effect that was partially prevented by co-silencing *PGI*. **(d)** Apoptotic death in *Cdh1*-silenced neurons was partially prevented by co-silencing either *cyclin B1* or *Pfkfb3* and was abolished by silencing both. Left histogram bar corresponds to control (luciferase) siRNA/shRNA.

manner, but had no effect on apoptosis in astrocytes (Supplementary Information, Fig. S3a). Expression of the kinase, but not the bisphosphatase domain of Pfkfb3 mimicked its effect on apoptosis in neurons (Fig. 2h). Silencing *PGI* abolished the apoptosis triggered by expression of either the full-length or the kinase domain of Pfkfb3 (Fig. 2h). The apoptosis in neurons resulting from expression of Pfkfb3 was caused by activation of the intrinsic apoptotic pathway, as demonstrated by the use of selective inhibitors of caspases (Supplementary Information, Fig. S3b). Thus, although overexpression of Pfkfb3 in neurons activates glycolysis, it concomitantly triggers apoptotic death.

To understand the reason(s) for apoptotic death of neurons following Pfkfb3-mediated activation of glycolysis, we decided to investigate whether such activation affected the rate of glucose utilization by the

**(e)** Transfection of full-length *Pfkfb3* cDNA in neurons significantly increased intracellular lactate concentrations, as assessed in GFP<sup>+</sup> neurons after sorting by flow cytometry; this effect was prevented by *PGI* siRNA. **(f, g)** Transfection of neurons with *Pfkfb3* induced apoptotic death in a concentration- **(f)** and time- **(g)** dependent manner. Apoptosis was assessed by the presence of annexin V<sup>+</sup>/7-AAD<sup>-</sup> cells measured by flow cytometry within the GFP<sup>+</sup> population. **(h)** Apoptotic death was also observed following transfection of *Pfkfb3* and of a truncated form of *Pfkfb3* containing the kinase domain. Transfection of the bisphosphatase Pfkfb3 domain did not affect apoptosis. The increase in apoptotic death in neurons caused by *Pfkfb3* or the kinase domain was prevented by silencing *PGI*. Results are mean ± s.e.m. ( $n = 3$ ). \* $P < 0.05$  versus the corresponding control; # $P < 0.05$  versus *Cdh1* siRNA **(d)**.

pentose-phosphate pathway (PPP), which is metabolically linked to glycolysis through the common intermediate glucose-6-phosphate (G6P)<sup>12</sup>. To establish whether modulation of glycolysis in neurons affects the rate of G6P oxidation through the PPP, neurons were transfected with *Pfkfb3* and GFP<sup>+</sup> cells were sorted by flow cytometry to assess PPP activity<sup>13,14</sup>. In control neurons the rate of glucose consumption through the PPP (Fig. 3a) was double that through glycolysis (Supplementary Information, Fig. S2a). *Pfkfb3* transfection inhibited glucose consumption through the PPP in neurons by about 50% (Fig. 3a); this effect was abolished by silencing *PGI*, indicating that such inhibition was a consequence of the activation of glycolysis (Fig. 3a). Overexpression of the full-length cDNA coding for glucose-6-phosphate dehydrogenase (G6PD; the rate-limiting step of the

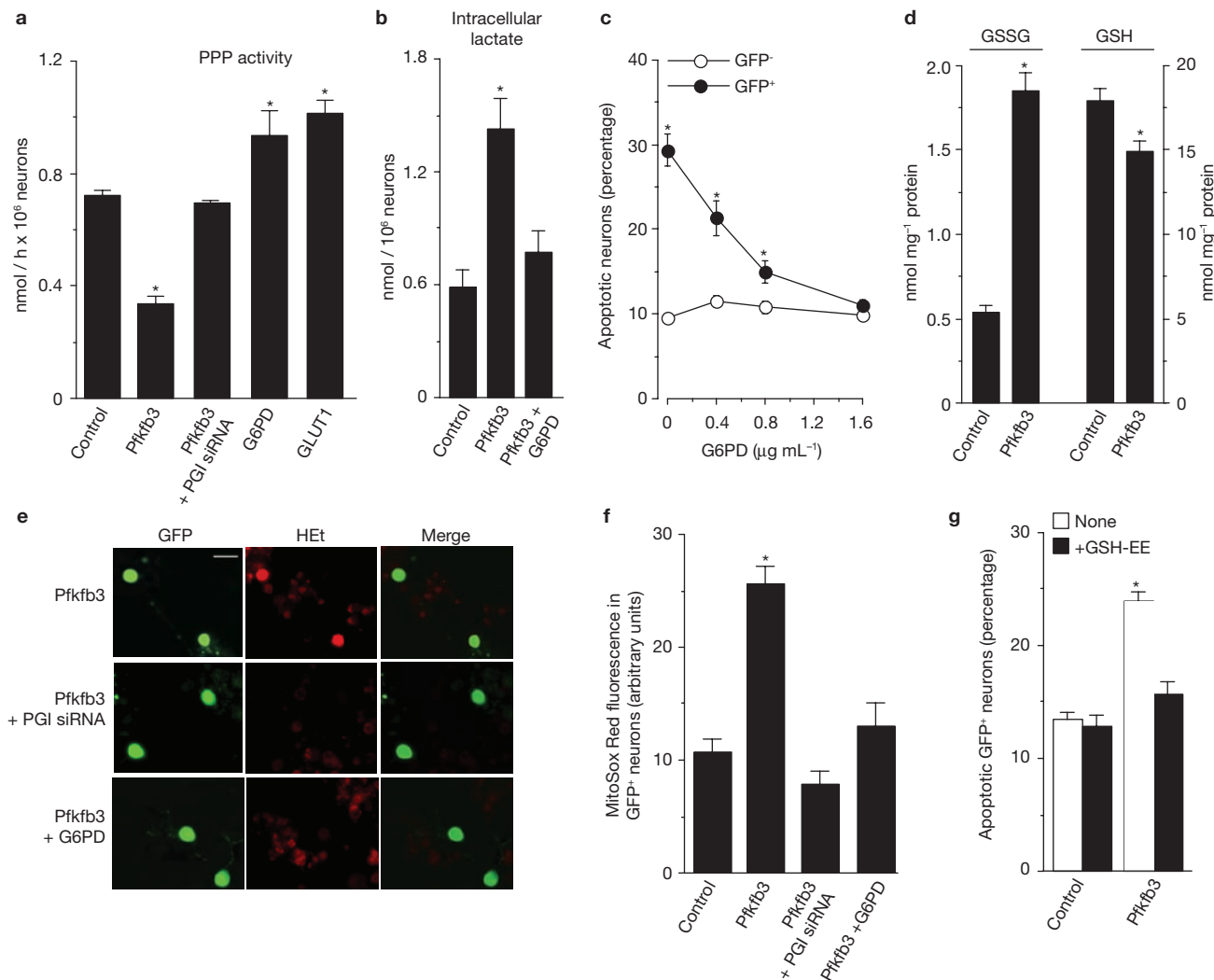


**Figure 3** Pfkfb3 expression in neurons triggers a decrease in glucose oxidation through the PPP, causing oxidative stress. **(a)** The rate of PPP activity, measured as the difference in the rates of oxidation of  $1^{-14}\text{C}$ - and  $6^{-14}\text{C}$ -glucose, was reduced in neurons transfected with *Pfkfb3*; this effect was prevented by *PGI* siRNA. Expression of a plasmid vector encoding the full-length cDNA of G6PD, or the glucose transporter GLUT1 increased the rate of  $1^{-14}\text{C}$ -glucose oxidation. These measurements were performed in GFP<sup>+</sup> cells sorted by flow cytometry. **(b)** Transfection of *Pfkfb3* in neurons resulted in increased intracellular lactate concentrations, an effect that was prevented by co-expressing G6PD. These measurements were performed in GFP<sup>+</sup> cells sorted by flow cytometry. **(c)** Neuronal apoptotic death (annexin V<sup>+</sup>/7-AAD<sup>+</sup>) caused by *Pfkfb3* expression was prevented by co-expression of G6PD. GFP<sup>+</sup> neurons indicate those efficiently transfected with the *Pfkfb3* cDNA construct, whereas GFP<sup>-</sup> neurons represent

PPP) significantly increased PPP activity, as did overexpression of the glucose transporter GLUT1 (Fig. 3a). Furthermore, the increase in lactate accumulation and the apoptosis induced by *Pfkfb3* transfection could be prevented by co-expression of G6PD (Fig. 3b, c). These results suggest that in neurons a significant proportion of G6P is directed towards the PPP and that *Pfkfb3* upregulation diverts it towards glycolysis. In astrocytes, however, despite considerable PPP activity<sup>14</sup>, there is substantial metabolism of glucose by glycolysis (Supplementary Information, Fig. S3c), consistent with the observed higher expression of both G6PD (Supplementary Information, Fig. S3d) and *Pfkfb3* (Fig. 1a) when compared with neurons.

those that were not transfected. **(d)** *Pfkfb3* expression in neurons followed by flow cytometric sorting of the GFP<sup>+</sup> neurons revealed an increase of about 4-fold in the intracellular concentration of GSSG and a corresponding decrease in reduced glutathione (GSH). **(e)** *Pfkfb3* expression in neurons increased the intensity of hydroethidine (HEt) fluorescence in the GFP<sup>+</sup> population, but not in the GFP<sup>-</sup> cells. Increased HEt fluorescence was abolished either by silencing *PGI* (*PGI* siRNA) or by G6PD expression. Scale bars, 20  $\mu\text{m}$ . **(f)** *Pfkfb3* expression in neurons increased the intensity of MitoSox fluorescence in the GFP<sup>+</sup> population, but not in the GFP<sup>-</sup> cells; this effect was abolished either by silencing *PGI* (*PGI* siRNA) or by G6PD expression. **(g)** Incubation of neurons with a plasma-permeable form of glutathione (glutathione ethyl ester, GSH-EE) prevented apoptotic death caused by *Pfkfb3* expression. Results are means  $\pm$  s.e.m. ( $n = 3$ ). \* $P < 0.05$  versus the corresponding control.

A major function of the PPP is the regeneration of reduced glutathione at the expense of NADPH( $\text{H}^{+}$ )<sup>7,13</sup> to provide neuroprotection<sup>14–16</sup>. We found that *Pfkfb3* transfection increased the oxidation of glutathione (Fig. 3d), indicating oxidative stress. We therefore measured the formation of reactive oxygen species (ROS). *Pfkfb3* expression enhanced the formation of ROS in neurons, an effect that was prevented either by silencing *PGI* or by co-expressing G6PD (Figs 3e, f; Supplementary Information, Fig. S3e). Moreover, incubation of neurons with a plasma-membrane-permeable form of glutathione (glutathione ethyl ester) prevented apoptosis caused by *Pfkfb3* expression (Fig. 3g). These results indicate that production of ROS in neurons

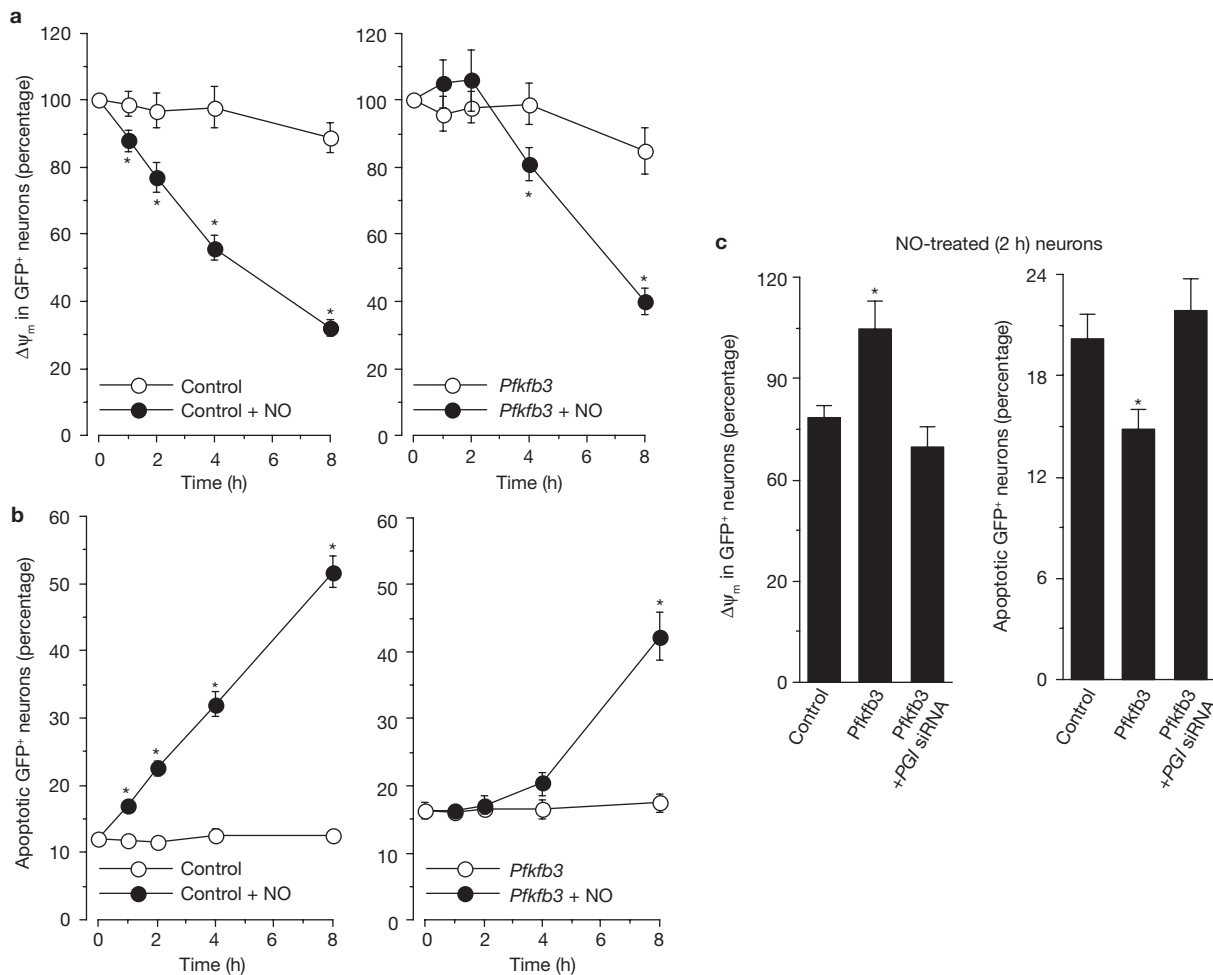


**Figure 4** Expression of *Pfkfb3* transiently protects neurons from loss of mitochondrial membrane potential ( $\Delta\Psi_m$ ) and apoptotic death triggered by nitric oxide (NO). **(a)** Primary neurons were transfected with control plasmid vector (left panel) or *Pfkfb3* (right panel) and then exposed to NO (released from the NO donor DETA–NONOate, 0.5 mM). NO triggered a rapid loss of  $\Delta\Psi_m$ , which was initially prevented in neurons transfected with *Pfkfb3*. **(b)** Apoptotic

transfected with *Pfkfb3* is consequent to the diversion of G6P from the PPP to glycolysis.

Treatment of neurons with the cytochrome *c* oxidase inhibitor nitric oxide (NO) is known to cause a marked drop in mitochondrial membrane potential ( $\Delta\Psi_m$ ), which is associated with an increase in apoptosis<sup>1</sup>. This does not occur in astrocytes because they are able to upregulate glycolysis and can use glycolytically generated ATP to maintain their  $\Delta\Psi_m$ . We therefore investigated the effect of *Pfkfb3* expression (at a concentration that did not itself cause apoptosis) on the response of neurons to inhibition of mitochondrial respiration. Treatment with NO, administered as DETA–NONOate, resulted in a marked drop in  $\Delta\Psi_m$  (Fig. 4a, left panel) and an increase in apoptosis (Fig. 4b, left panel). Transfection with *Pfkfb3* transiently delayed, but did not prevent the onset of the NO-induced fall in  $\Delta\Psi_m$  (Fig. 4a, right panel) and apoptosis (Fig. 4b, right panel), an effect that could be abolished by silencing *PGI* (Fig. 4c). Similar results were obtained when antimycin A was used to inhibit the electron transport chain (Supplementary Information, Fig. S3f–h). Thus, following cellular stress induced by inhibition of mitochondrial respiration, transfection of neurons with *Pfkfb3* activates glycolysis; however

death was assessed in neurons treated as in **a**. NO triggered apoptotic death of neurons transfected with control plasmid vector (left panel). However, in neurons transfected with *Pfkfb3*, the effect of NO was delayed for 4 h (right panel). **(c)** The protective effect of *Pfkfb3* against NO-mediated loss of  $\Delta\Psi_m$  (left panel) and apoptotic death (right panel) was prevented by *PGI* siRNA. Results are means  $\pm$  s.e.m. ( $n = 3$ ). \* $P < 0.05$  versus the corresponding control.

this produces only limited protection, as glycolysis diverts glucose away from the PPP, resulting in oxidative stress and death.

Thus, *Pfkfb3* is degraded by an active mechanism that seems to be physiological as the enzyme is absent in neurons in the normal rat brain. This explains the lower rate of glycolytic metabolism in neurons than in astrocytes<sup>1</sup>. Furthermore, under stress conditions, this mechanism prevents upregulation of glycolysis, which is normally observed in astrocytes as part of their defence response<sup>2</sup>. Indeed, we show that enhancement of glycolysis in neurons leads to their apoptotic death from oxidative stress, consequent to a decrease in the regeneration of reduced glutathione.

Our results also suggest that neuronal consumption of glucose by the PPP to maintain their antioxidant status may take priority over the use of glucose to fulfill their bioenergetic requirements, which can be met by other sources. Increasing evidence indicates that neurons can use lactate generated by astrocytes to produce energy<sup>17</sup> and that this is not a uniform process but varies as a result of glutamatergic activation<sup>18</sup>. The fact that *Pfkfb3* is subject to proteasomal degradation suggests that this mechanism is amenable to modulation, under conditions that now

require investigation. Indeed, it is likely that the increased use of lactate by neurons is coupled to an increase in their regeneration of reduced glutathione from glucose. Regulation of Pfkfb3 stability by the APC/C-Cdh1 pathway that we now describe might underlie this process. □

## METHODS

Methods and any associated references are available in the online version of the paper at <http://www.nature.com/naturecellbiology>

*Note: Supplementary Information is available on the Nature Cell Biology website.*

## ACKNOWLEDGEMENTS

This work was supported by Ministerio de Ciencia e Innovación (SAF2007-61492 and Consolider-Ingenio CSD2007-00020, Spain), Instituto de Salud Carlos-III (FIS06/0794 and Renevas), and Junta de Castilla y León (SA066A07 and Red de Terapia Celular y Medicina Regenerativa). We would like to thank H. Yamano for valuable help with the APC/C-Cdh1 activity assays, Carmela Gómez-Rodríguez for immunohistochemistry experiments, M. Resch for technical assistance and A. Higgs for critical evaluation of this paper.

## AUTHOR CONTRIBUTIONS

A.H.M., E.F. and C.M. performed the experiments; A.A. and J.P.B. analysed the data; A.A., S.M. and J.P.B. planned the experiments and wrote the paper.

## COMPETING INTERESTS

The authors declare that they have no competing financial interest.

Published online at <http://www.nature.com/naturecellbiology/>

Reprints and permissions information is available online at <http://npg.nature.com/reprintsandpermissions/>

- Almeida, A., Almeida, J., Bolaños, J. P. & Moncada, S. Different responses of astrocytes and neurons to nitric oxide: the role of glycolytically-generated ATP in astrocyte protection. *Proc. Natl Acad. Sci. USA* **98**, 15294–15299 (2001).
- Almeida, A., Moncada, S. & Bolaños, J. P. Nitric oxide switches on glycolysis through the AMP protein kinase and 6-phosphofructo-2-kinase pathway. *Nature Cell Biol.* **6**, 45–51 (2004).

- Hue, L. & Rider, M. H. Role of fructose 2, 6-bisphosphate in the control of glycolysis in mammalian tissues. *Biochem. J.* **245**, 313–324 (1987).
- Van Schaftingen, E., Lederer, B., Bartrons, R. & Hers, H. G. A kinetic study of pyrophosphate: fructose-6-phosphate phosphotransferase from potato tubers. Application to a microassay of fructose 2, 6-bisphosphate. *Eur. J. Biochem.* **129**, 191–195 (1982).
- Uyeda, K. Phosphofructokinase. *Adv. Enzymol. Relat. Areas Mol. Biol.* **48**, 193–244 (1979).
- Sudakin, V. *et al.* The cycosome, a large complex containing cyclin-selective ubiquitin ligase activity, targets cyclins for destruction at the end of mitosis. *Mol. Biol. Cell* **6**, 185–197 (1995).
- Kletzien, R. F., Harris, P. K. W. & Foellmi, L. A. Glucose-6-phosphate dehydrogenase: a housekeeping enzyme subject to tissue-specific regulation by hormones, nutrients, and oxidant stress. *FASEB J.* **8**, 174–181 (1994).
- Riera, L. *et al.* Regulation of ubiquitous 6-phosphofructo-2-kinase by the ubiquitin-proteasome proteolytic pathway during myogenic C2C12 cell differentiation. *FEBS Lett.* **550**, 23–29 (2003).
- Pfleger, C. M. & Kirschner, M. W. The KEN box: an APC recognition signal distinct from the D box targeted by Cdh1. *Genes Dev.* **14**, 655–65 (2000).
- Visintin, R., Prinz, S. & Amon, A. CDC20 and CDH1: a family of substrate-specific activators of APC-dependent proteolysis. *Science* **278**, 460–463 (1997).
- Almeida, A., Bolanos, J. P. & Moreno, S. Cdh1/Hct1-APC is essential for the survival of postmitotic neurons. *J. Neurosci.* **25**, 8115–8121 (2005).
- Cohen, S. S. Studies on the distribution of the oxidative pathway of glucose-6-phosphate utilization. *Biol. Bull.* **99**, 369 (1950).
- Hothersall, J. S., Baquer, N. Z., Greenbaum, A. L. & McLean, P. Alternative pathways of glucose utilization in brain. Changes in the pattern of glucose utilization in brain during development and the effect of phenazine methosulphate on the integration of metabolic routes. *Arch. Biochem. Biophys.* **198**, 478–492 (1979).
- Garcia Nogales, P., Almeida, A. & Bolaños, J. P. Peroxynitrite protects neurons against nitric oxide-mediated apoptosis. A key role for glucose-6-phosphate dehydrogenase activity in neuroprotection. *J. Biol. Chem.* **278**, 864–874 (2003).
- Ben-Yoseph, O., Boxer, P. A. & Ross, B. D. Assessment of the role of the glutathione and pentose phosphate pathways in the protection of primary cerebrocortical cultures from oxidative stress. *J. Neurochem.* **66**, 2329–2337 (1996).
- Vaughn, A. E. & Deshmukh, M. Glucose metabolism inhibits apoptosis in neurons and cancer cells by redox inactivation of cytochrome c. *Nature Cell Biol.* **10**, 1477–1483 (2008).
- Tsacopoulos, M. & Magistretti, P. J. Metabolic coupling between glia and neurons. *J. Neurosci.* **16**, 877–885 (1996).
- Pellerin, L. *et al.* Activity-dependent regulation of energy metabolism by astrocytes: an update. *Glia* **55**, 1251–1262 (2007).

## METHODS

**Cell culture.** Cortical neurons or astrocytes in primary culture were prepared from fetal (E16) and neonatal (P0) Wistar rats, respectively. Cells were seeded ( $2.5 \times 10^5$  cells/cm $^2$ ) in DMEM (Sigma) supplemented with 10% (v/v) fetal calf serum (FCS, Roche Diagnostics) and incubated at 37 °C in a humidified 5% CO $_2$ -containing atmosphere. For neuronal cultures, 48 h after plating the medium was replaced with DMEM supplemented with 5% horse serum (Sigma) and with 20 mM D-glucose. On day 4 cytosine arabinoside (10  $\mu$ M) was added to prevent non-neuronal proliferation. Cells were used by day 6 (neurons) or 12 (astrocytes). Enrichment was about 99% (neurofilament) or about 85% (glial-fibrillary acidic protein) in neurons and astrocytes, respectively. Most other cells in astrocytic cultures were microglia and progenitor cells<sup>11</sup>.

**Plasmid constructions.** The full-length *Pfkfb3* cDNA (1563 bp; accession number BAA21754) was obtained by RT-PCR using total RNA from rat astrocytes as the template. The sense and antisense oligonucleotides and RT-PCR conditions are described in Supplementary Information Methods. Full-length rat G6PD cDNA<sup>14</sup>, rat *GLUT1* cDNA<sup>19</sup> and human *Cdh1* cDNA<sup>11</sup> were also used. For small hairpin RNA (shRNA) expression, pSuper-based vectors were used<sup>20</sup>.

**Site-directed mutagenesis.** To mutate the KEN-box to AAA in *Pfkfb3* cDNA, we used the QuikChange XL site-directed mutagenesis kit (Stratagene) using the following forward and reverse primers, respectively: 5'-ATCCTTCATTGCGCAGCTGACTTCAAGGC-3' and 5'-ATGCCTGAAGTCAGCTGCTGCGGAAATGAAGG-3' (mutated nucleotides underlined).

**Anti-*Pfkfb3* antibody.** This was generated by immunization of rabbits with the synthetic peptide <sup>508</sup>MRSPRSGAESSQKH<sup>521</sup>-C, as described in the Supplementary Information Methods.

**RT-PCR.** To identify the *Pfkfb* isoforms and *Pfkfb3* splice variants expressed in neurons, total RNA samples were amplified using the oligonucleotides and conditions described in the Supplementary Information Methods.

**RNA interference.** Using previously reported criteria<sup>21,22</sup>, two sequences, 5'-CCTTACCAAGACGTAGTGTT-3' (nucleotides 1248–1266) and 5'-GCAAAGCTATCACGGACAT-3' (nucleotides 503–521), were designed to target *PGI* by small interfering RNA (siRNA). However, the former was most effective at decreasing PGI protein in preliminary experiments (data not shown). Previously reported siRNA/ shRNA sequences for *Cdh1* (5'-TGAGAAGTCTCCCAGTCAG-3', nucleotides 235–253; ref. 20), *cyclin B1* (5'-GATGGAGCTGATCCAAAC-3', nucleotides 478–496; ref. 11) and *Pfkfb3* (5'-AAAGCCTCGCATCACAGC-3', nucleotides 1908–1926; ref. 2) were used. In all cases, a siRNA or shRNA against luciferase (5'-CTGACCGGAAATCTCGATT-3') was used as a control<sup>3</sup>.

**Cell treatments.** Preliminary experiments using 20–100 nM of the siRNAs (Thermo Fisher Scientific) showed a concentration-dependent effect, and only the results using 100 nM are shown. Transfection of cells with plasmid vectors was carried out using 0.4–1.6  $\mu$ g ml $^{-1}$  of the plasmids. All transfections were performed using lipofectamine 2000 (Invitrogen) according to the manufacturer's instructions. After 6 h, the medium was removed and cells were further incubated for the indicated times in the presence of culture medium. Neuronal siRNA transfections were performed at day 3 *in vitro*, although experiments were performed at days 5 or 6; plasmid transfections were performed at day 5 *in vitro*. Experiments with the proteasome inhibitors MG-132 and lactacystine (10  $\mu$ M; Calbiochem) were performed at day 6 *in vitro* and cells collected after 1 h. Glutathione ethyl ester (5 mM; Sigma), or the caspase inhibitors Z-VAD-FMK, Z-DEVD-FMK, Z-IETD-FMK, Z-VDVAD-FMK and Z-LEHD-FMK (50  $\mu$ M; Calbiochem) was added to the cell medium 6 h after transfection. To expose the cells to controlled amounts of NO, cells were incubated in DMEM containing DETA-NO ((Z)-1-[2-aminoethyl-N-(2-aminoethyl)amino] diazen-1-iun-1,2-diolate; Alexis Corporation) at 0.5 mM, which is the concentration seen to release about 1.4  $\mu$ M of NO continuously for about 18 h at 37 °C, as measured by an NO-sensitive electrode (World Precision Instruments). To ensure immediate exposure of the cells to NO, all DETA-NO-containing solutions were always pre-incubated in DMEM at 37 °C for 30 min before addition to the cells<sup>1</sup>. Antimycin A was used at 5  $\mu$ M for 30 min, neurons were washed and further incubated in DMEM for the indicated times.

**Flow cytometric analysis of apoptotic cell death.** APC-conjugated annexin-V and 7-amino-actinomycin D (7-AAD) (Becton Dickinson Biosciences) were used to determine quantitatively the percentage of apoptotic neurons by flow cytometry. Cells were stained with annexin V-APC and 7-AAD, according to the manufacturer's instructions, and were analysed on a FACScalibur flow cytometer (15 mW argon ion laser tuned at 488 nm; CellQuest software, Becton Dickinson Biosciences). GFP $^+$  and GFP $^-$  cells were analysed separately, and the annexin V-APC-stained cells that were 7-AAD-negative were considered to be apoptotic<sup>2</sup>.

**Cell sorting.** Neurons were transfected and, at the indicated time-points, carefully detached from the plates using 1 mM tetrasodium EDTA in PBS. Cell sorting was performed by flow cytometry in a FACScalibur flow cytometer (Becton Dickinson Biosciences). Distinction between the two cells subsets was based on expression of the GFP protein or the annexin V/7-AAD staining. The purity of the sorted fraction was 98%  $\pm$  1.6% (range, 95%–99.5%).

**Flow cytometric analysis of mitochondrial membrane potential ( $\Delta\psi_m$ ).** This was assessed in the GFP $^+$ -stained cells using a MitoProbe DiC1(5) assay kit for flow cytometry (Molecular Probes Europe BV) according to the manufacturer's instructions. We used the FL1 and FL4 channels of a FACScalibur flow cytometer (15 mW argon ion laser tuned at 488 nm; CellQuest software, Becton Dickinson Biosciences).  $\Delta\psi_m$  values were expressed as percentages, and the mitochondrial uncoupler oligomycin (10  $\mu$ M, 10 min; Sigma) was used to define the 0%  $\Delta\psi_m$  values.

**Detection of reactive oxygen species (ROS).** This was carried out using both the dihydroethidine and MitoSox-Red methods (Invitrogen). Neurons were incubated in PBS containing dihydroethidine (10  $\mu$ M; Molecular Probes) at 37 °C in the dark for 45 min; excess dihydroethidine was removed and the amount of oxidized product (ethidium) was determined by fluorescence (510–560 nm) microscopy. For the MitoSox-Red method, neurons were incubated with MitoSox-Red (2  $\mu$ M) for 30 min, washed with PBS and fluorescence assessed by flow cytometry.

**Determination of the glycolytic flux.** This was measured by two different methods, namely the rate of 6-<sup>14</sup>C-glucose conversion to <sup>14</sup>C-lactate and the rate of <sup>3</sup>H<sub>2</sub>O production from 3-<sup>3</sup>H-glucose, as described in the Supplementary Information Methods.

**Determination of activity of the pentose-phosphate pathway (PPP).** This was measured in flow cytometric GFP $^+$ -sorted neurons, prepared as indicated in the Supplementary Information Methods, by assessing the difference between <sup>14</sup>CO<sub>2</sub> production from 1-<sup>14</sup>C-glucose, which decarboxylates through the 6-phosphogluconate dehydrogenase-catalysed reaction, and that of 6-<sup>14</sup>C-glucose, which decarboxylates through the tricarboxylic acid cycle<sup>13,23</sup>.

**Metabolite determinations.** Glucose G6P, F6P, F1,6P<sub>2</sub>, F2,6P<sub>2</sub>, lactate and total and oxidized glutathione concentrations were measured as described in the Supplementary Information Methods.

**APC/C ubiquitin ligase activity, northern blotting, western blotting and immunohistochemistry.** These procedures were carried out as described in the Supplementary Information Methods.

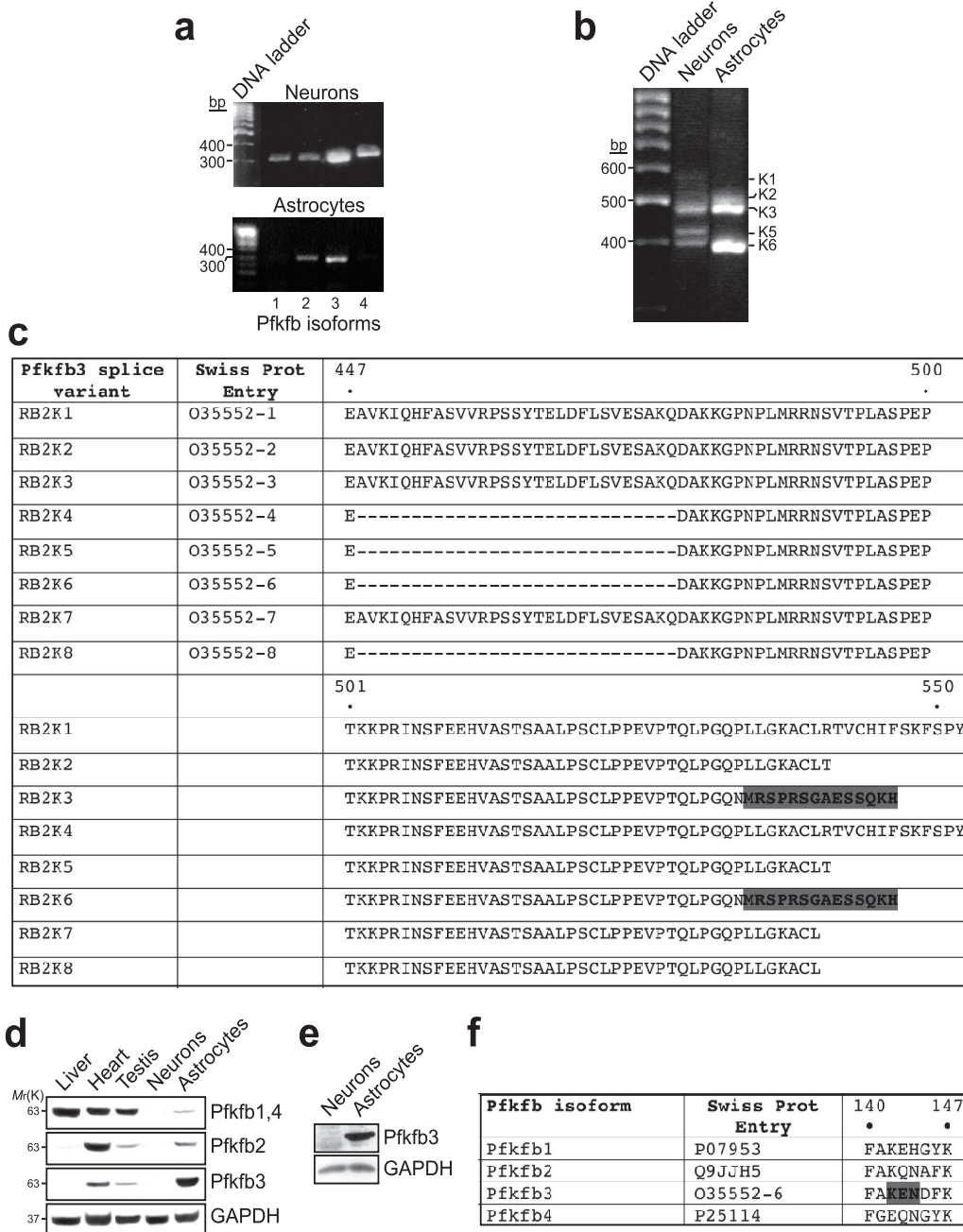
**Protein determinations.** Protein concentrations were determined in the cell suspensions, lysates or in parallel cell culture incubations after solubilization with 0.1 M NaOH. Protein concentrations were determined as described<sup>24</sup> using bovine serum albumin as a standard.

**Statistical analysis.** Measurements from individual cultures were always carried out in triplicate. The results are expressed as mean  $\pm$  s.e.m. for three different culture preparations. Statistical analysis of the results was performed by one-way analysis of variance, followed by the least significant difference multiple range test. In all cases,  $P < 0.05$  was considered significant.

19. Cidat, P., Almeida, A. & Bolaños, J. P. Inhibition of mitochondrial respiration by nitric oxide rapidly stimulates cytoprotective GLUT3-mediated glucose uptake through 5'-AMP-activated protein kinase. *Biochem. J.* **384**, 629–636 (2004).
20. Brummelkamp, T. R., Bernards, R. & Agami, R. A system for stable expression of short interfering RNAs in mammalian cells. *Science* **296**, 550–553 (2002).

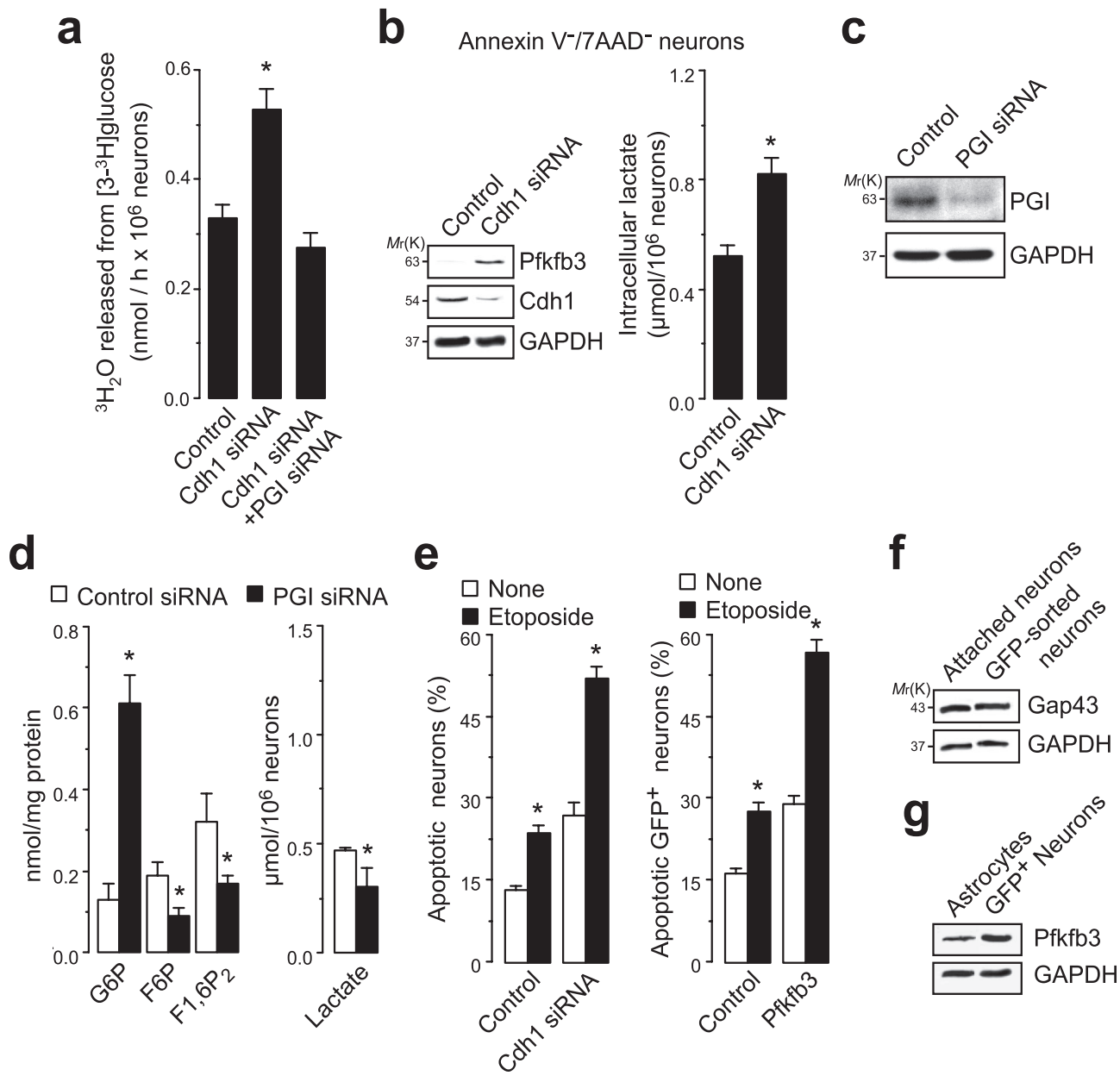
21. Reynolds, A. *et al.* Rational siRNA design for RNA interference. *Nature Biotechnol.* **22**, 326–330 (2004).
22. Ui-Tei, K. *et al.* Guidelines for the selection of highly effective siRNA sequences for mammalian and chick RNA interference. *Nucleic Acids Res.* **32**, 936–948 (2004).
23. Larrabee, M. G. Evaluation of the pentose phosphate pathway from  $^{14}\text{CO}_2$  data. Fallibility of a classic equation when applied to non-homogeneous tissues. *Biochem. J.* **272**, 127–132 (1990).
24. Lowry, O. H., Rosebrough, N. J., Lewis-Farr, A. & Randall, R. J. Protein measurement with the Folin phenol reagent. *J. Biol. Chem.* **193**, 265–275 (1951).

DOI: 10.1038/ncb1881



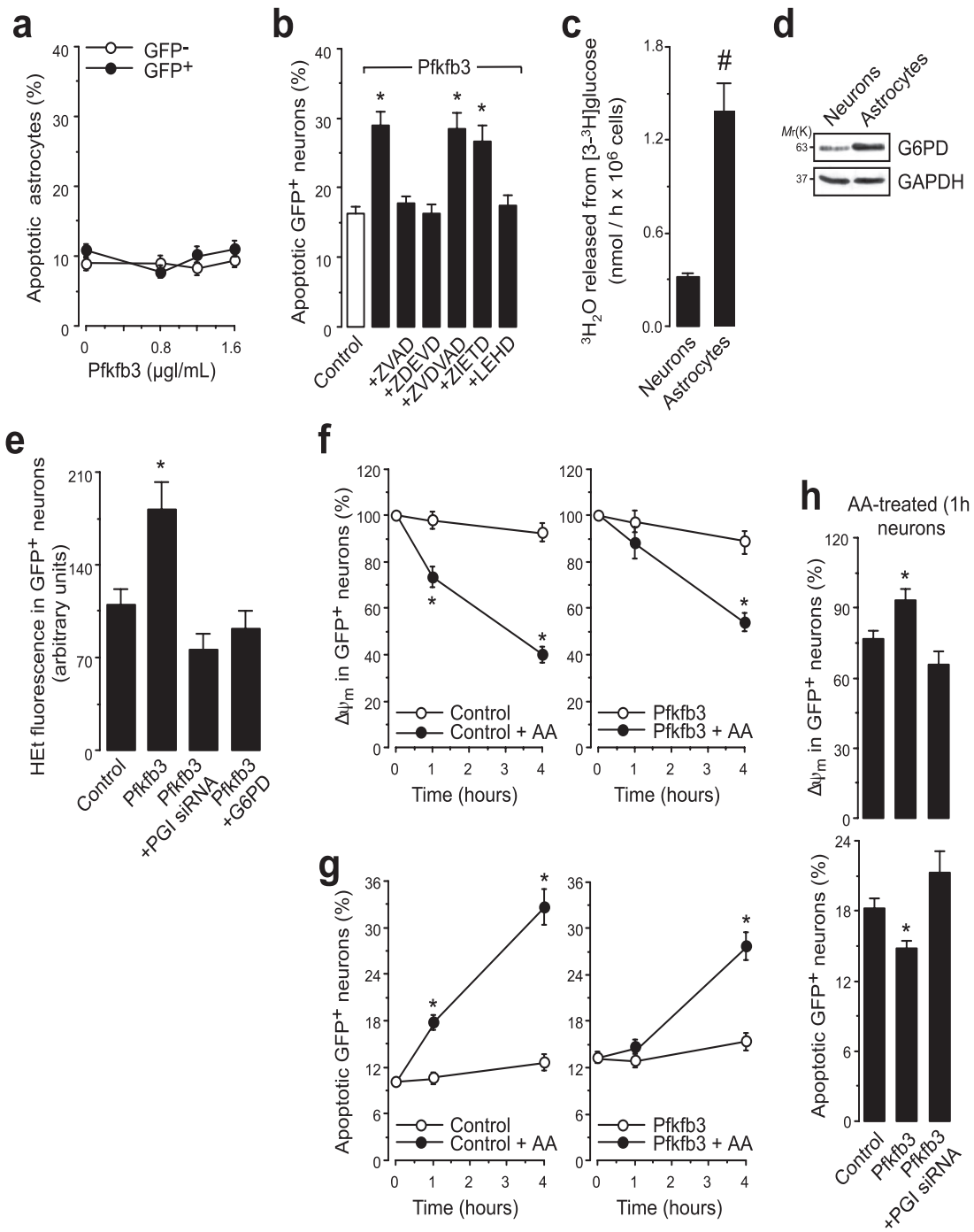
**Figure S1** (a) Reverse-transcriptase polymerase-chain reaction (rtPCR) was carried out in total RNA samples from rat cortical neurons and astrocytes to identify the four different Pfkfb isoforms. Isoform 3 (Pfkfb3) was found to be the most abundant in both cell types. (b) rtPCR was performed in total RNA samples obtained from rat cortical neurons or astrocytes to identify the most abundant mRNA splice variants (K1 to K8) expressed. In neurons, the expression of K3, K5 and K6 was comparable, whereas in astrocytes K6, followed by K3 was expressed the most. K7 and K8 were not detectable in either cell type (not shown). (c) Aminoacid sequences of the C-terminal

domains of the eight splice variants described for the rat Pfkfb3. The epitope used for antibody production is highlighted. (d) Neurons do not express any Pfkfb isoform, whereas astrocytes express Pfkfb3, Pfkfb2 and Pfkfb1,4. (e) Western blotting against Pfkfb3 using a commercial antibody that does not distinguish among different splice variants (catalogue number sc-10091, Santa Cruz Biotechnologies; see Supplementary Methods) confirms the lack of Pfkfb3 protein in neurons. (f) 140-147 aminoacid sequence of Pfkfb isoforms showing the presence of a KEN box in Pfkfb3 but not in the other isoforms.



**Figure S2** (a) Knockdown of Cdh1 increased the rate of  ${}^3\text{H}_2\text{O}$  released from  $[{}^3\text{H}]\text{glucose}$ , an index of glucose utilization through Pfk1; this effect was prevented by co-silencing PGI. (b) Cdh1 silencing increased Pfkfb3 protein and lactate in the surviving subpopulation of neurons (annexin V-/7-AAD $^-$ ). (c) Primary cortical neurons were transfected with PGI siRNA at 3 days *in vitro*. Three days later, western blotting showed that PGI was knocked down by the siRNA procedure. (d) To further validate the effectiveness of the PGI siRNA procedure, both PGI substrate (glucose-6-phosphate; G6P) and product (fructose-6-phosphate; F6P), as well as the Pfk1 product fructose-1,6-bisphosphate (F1,6P<sub>2</sub>), and lactate, were measured in primary cortical neurons transfected with PGI siRNA under the conditions described in the legend to panel (c). PGI siRNA resulted in accumulation of G6P and a decrease in F6P, thus confirming inhibition of the PGI-catalyzed reaction by PGI siRNA. The decrease in F1,6P<sub>2</sub> and lactate concentrations observed

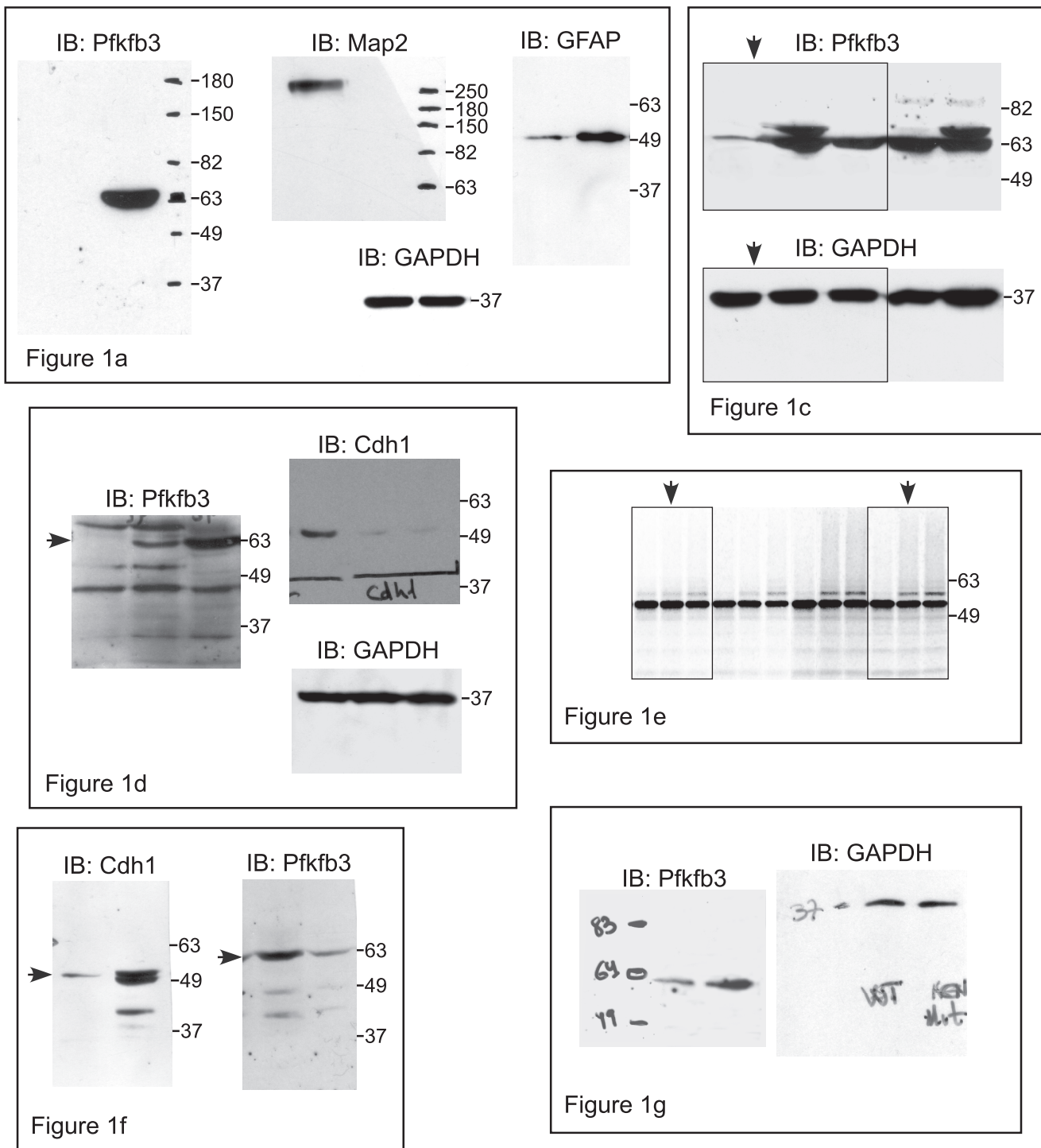
after PGI siRNA treatment also suggests that glycolysis in neurons is not supported by redirection of G6P through the non-oxidative branch of the PPP. (e) Cdh1 silencing (left panel) or over-expression of Pfkfb3 (right panel) increased neuronal apoptosis triggered by etoposide. (f) To test whether detachment of neurons from the plates resulted in a loss of neurites and/or axons, western blotting against the synaptic protein Gap43 was performed in neurons lysed on plates or lysed after cell sorting. The presence of equivalent amounts of Gap43 in the attached and the cell-sorted neurons shows that collection of the neurons followed by flow cytometric sorting does not cause a loss of the neurites/axons. (g) Moderate over-expression of Pfkfb3 cDNA in neurons followed by cell sorting revealed the accumulation of Pfkfb3 in amounts approximately 1-5-fold higher than those found in astrocytes, as assessed by densitometry. Results are means  $\pm$  S.E.M (n=3). \*p<0.05 versus the corresponding control.



**Figure S3** (a) Over-expression of Pfkfb3 does not cause apoptotic cell death in astrocytes. (b) The apoptotic death of primary neurons caused by Pfkfb3 expression was prevented by inhibitors of caspases (ZVAD), caspase-3 (ZDEVD) and caspase-9 (LEHD), but not by inhibitors of caspase-8 (ZVDVAD) or caspase-2 (ZIETD). (c) The rate of  ${}^3\text{H}_2\text{O}$  released from  $[{}^3\text{H}]$ glucose (an index of glucose consumption through Pfk1) was about 4.5-times higher in astrocytes than in neurons. The rate of conversion of  $[{}^3\text{H}]$ glucose into  ${}^3\text{H}_2\text{O}$  was expressed per  $10^6$  cells in order to facilitate comparison of glucose consumed through Pfk1 (this panel) with that consumed through the PPP (see Fig. 3a); 10<sup>6</sup> astrocytes contained 0.80 mg of protein, and 10<sup>6</sup> neurons contained 0.70 mg of protein. (d) Endogenous levels of glucose-6-phosphate dehydrogenase (G6PD) are approximately 2.5-fold higher in astrocytes than in neurons, as assessed by densitometry. (e) Quantitation of

HEt fluorescence (see Fig. 3e) after Pfkfb3 expression in neurons, showing that the increased HEt fluorescence was abolished either by PGI silencing (PGI siRNA) or G6PD expression. (f) Primary neurons were transfected with control plasmid vector (left panel) or Pfkfb3 (right panel) and then exposed to antimycin A (AA). AA triggered a rapid loss of  $\Delta\psi_m$ , which was initially prevented in neurons transfected with Pfkfb3. (g) Apoptotic death was assessed in neurons treated as in (f). AA triggered apoptotic death of neurons transfected with control plasmid vector (left panel). However, in neurons transfected with Pfkfb3 the effect of AA was delayed (right panel). (h) The protective effect of Pfkfb3 against AA-mediated loss of  $\Delta\psi_m$  (upper panel) and apoptotic death (lower panel) was prevented by PGI siRNA. Results are means  $\pm$  S.E.M (n=3). \*p<0.05 versus the corresponding control; #p<0.05 versus neurons.

## SUPPLEMENTARY INFORMATION



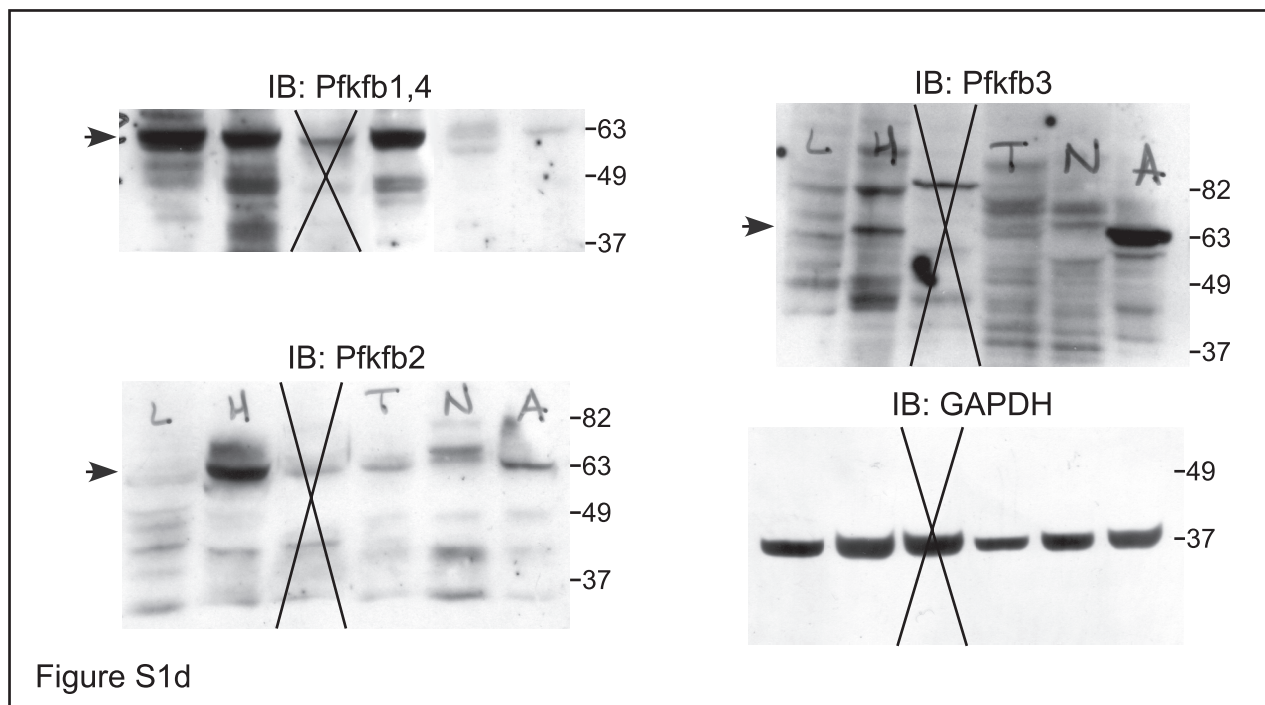


Figure S1d

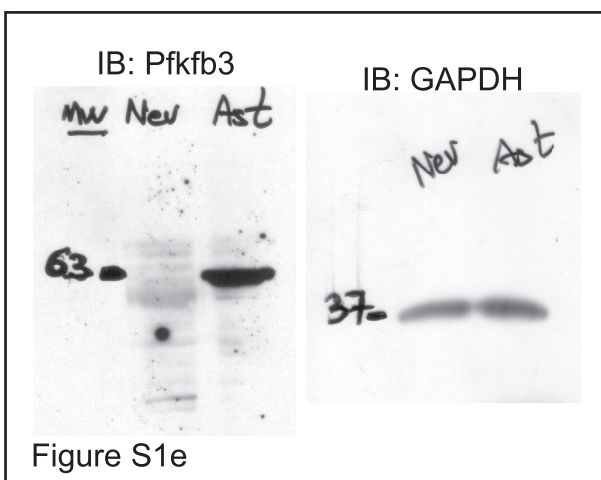


Figure S1e

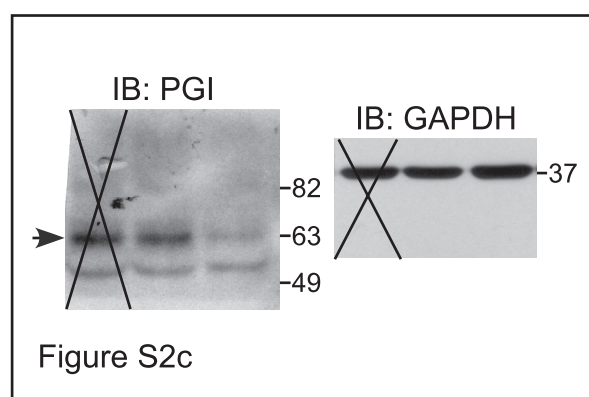


Figure S2c

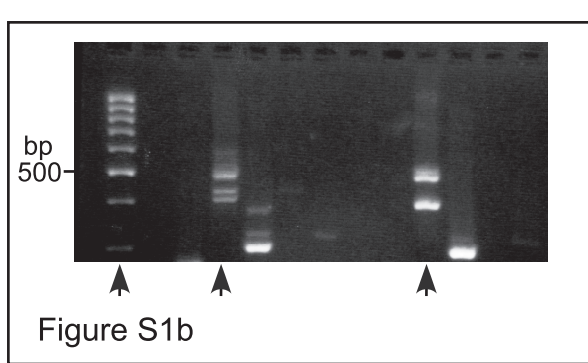


Figure S1b

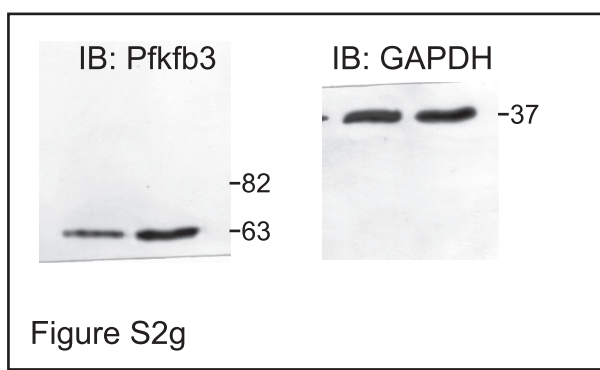


Figure S2g

Figure S4 continued

## Supplementary Methods

*Oligonucleotides and rtPCR conditions to amplify Pfkfb3.* The sense and antisense oligonucleotides used to amplify the Pfkfb3 full length cDNA were 5'-GTCGCCGAATACAGCAACGAAGATG-3' and 5'-GAACCCCTACTCAGCATCAGTG-3', respectively. To obtain the Pfkfb3 kinase domain (735 bp) we used the following forward and reverse oligonucleotides, respectively: 5'-GTCGCCGAATACAGCAACGAAGATG-3' and 5'-TCCGGGGAAATCCGGCTACTGCACGTGGATGTTCA-3'. To obtain the Pfkfb3 bisphosphatase domain (828 bp) we used 5'-CCCCGGACCATCTACCTGTGT and 5'-GAACCCCTACTCAGCATCAGTG-3'. Reverse transcription was performed at 48 °C for 50 min, and PCR conditions were 10 min at 94 °C, 1 min at 94 °C (35 cycles), 1 min at 59,7 °C, and 2 min at 68 °C. Final extension was carried out for 10 min at 68 °C. The cDNA products were purified, inserted in the *Eco*RI site of pIRE2-EGFP mammalian expression vector (Invitrogen) and sequenced. This construction was functional, as judged by the increased F2,6P<sub>2</sub> concentrations obtained in HEK293T cells (in nmol/mg protein, control, 80±5; Pfkfb3, 130±11; n=3). HEK293T cells were incubated in DMEM containing 10% FCS and seeded at 10<sup>5</sup> cells/cm<sup>2</sup> 24 h before the experiments were carried out.

*Antibodies against Pfkfb3.* A polyclonal antibody against Pfkfb3 was obtained by rabbit immunization with 100 ng of the Keyhole Limpet haemocyanin-coupled synthetic peptide (Thermo Fisher Scientific, Waltham, MA, USA) <sup>508</sup>MRSPRSQGAESSQKH<sup>521</sup>-C, which is common to the translational products of the Pfkfb3 mRNA splice variants K3 and K6. Antisera were purified by affinity chromatography using columns of cyanogen-bromide-activated sepharose coupled to the peptide. The specificity of the antibody was tested by dot blotting against the peptides at a dilution of 1:20,000. Since this antibody does not recognise the other translational products of the rat Pfkfb3, we also used a commercial anti-Pfkfb3 antibody raised against a C-terminal region of the human Pfkfb3 (Protein Accession Q16875; catalogue number sc-10091, Santa Cruz Biotechnology, Santa Cruz, CA. U.S.A.). This antibody cross-reacts with human and rat Pfkfb3 (<http://www.scbt.com/datasheet-10091-pfk-2-br-pl-1-13-antibody.html>) and therefore recognizes a region that is shared by all translational products of the rat K1 to K8 Pfkfb3 mRNA splice variants.

*Reverse transcription-polymerase chain reaction (rtPCR).* To identify the Pfkfb isoforms expressed in neurons, total RNA samples from rat cultured neurons were amplified using the following forward and reverse oligonucleotides, respectively: 5'-CAGATGAGCTGCCCTATCTCAAGT-3' and 5'-AGGTAGGGCACTCTCAGGCCATAG-3' for Pfkfb1; 5'-CGTCCTCGTTATCTCTCAC-3' and 5'-CCCAACACTGTAATTCTTGGAC-3' for Pfkfb2; 5'-CCAGCCTTTGACCCTGATAAATG-3' and 5'-TCCACACGCGGAGGTCTTCAGAT-3' for Pfkfb3, and 5'-ACCACTACCCGCTGGAGTTG-3' and 5'-GTCTGTCTCGGTGTGTTCA-3' for Pfkfb4. RT-PCR conditions were 50 min at 48 °C for reverse transcription; 10 min at 94 °C; 35 cycles of 1 min at 94 °C, 1 min at 58 °C, and 30 seconds at 68 °C; final extension was carried out for 10 min at 68 °C. To identify the eight Pfkfb3 alternative splice variants<sup>1</sup> in rat neurons and astrocytes, total RNA samples of these cells were amplified using the following forward and reverse oligonucleotides, respectively: 5'-CTAGCCTACTTCCTTGACAAG-3' and 5'-GTGACAGACAGTTCGTAGACAGG-

3' (for both K1 and K4); 5'-CTAGCCTACTTCCTTGACAAG-3' and 5'-GAACCCCTACTTCAGCATCAGTG-3' (for K1 to K6); 5'-CTAGCCTACTTCCTTGACAAG-3' and 5'-GGAGACCAAAAGGGCCAACAAGC-3' (for K7 and K8). Reverse transcription was carried out at 48 °C for 50 min, and PCR conditions were 10 min at 94 °C; 1 min at 94 °C (35 cycles); 45 seconds at 56.8 °C and 45 seconds at 68 °C; final extension was carried out for 10 min at 68 °C.

*Preparations of cells for the measurement of PPP and glycolytic fluxes.* Suspensions of known amounts of cells (~1-2 x 10<sup>5</sup> cells) obtained from sorting or culture were incubated in sealed vials containing a central well, which was used for <sup>14</sup>CO<sub>2</sub> or <sup>3</sup>H<sub>2</sub>O trapping, in the presence of 1 µCi of D-[1-<sup>14</sup>C]glucose (for PPP determinations), D-[6-<sup>14</sup>C]glucose (1 µCi for glycolytic flux determinations; 5 µCi for PPP determinations) or 5 µCi of D-[3-<sup>3</sup>H]glucose (for glycolytic flux determinations) in a Krebs-Henseleit buffer (11 mM Na<sub>2</sub>HPO<sub>4</sub>, 122 mM NaCl, 3.1 mM KCl, 0.4 mM KH<sub>2</sub>PO<sub>4</sub>, 1.2 mM MgSO<sub>4</sub>, 1.3 mM CaCl<sub>2</sub>; pH 7.4) containing 5 mM D-glucose at 37 °C. We used this buffer instead of the culture medium because of its simpler composition. In addition, we used suspended, rather than plated cells because cell-sorted neurons do not attach when re-plated, and also because most <sup>14</sup>CO<sub>2</sub> or <sup>3</sup>H<sub>2</sub>O released from cells would be lost from the non-hermetically-sealed Petri dishes. In order to ensure an adequate O<sub>2</sub> supply for oxidative metabolism by the cells throughout the 90 minute incubation period, the gas phase in the vials containing the cells was supplied with extra O<sub>2</sub> before the vials were sealed.

*Determination of the glycolytic flux.* Cells were incubated as indicated in the previous section, and the reaction was stopped after 90 min with either NaOH (0.06 M) (for <sup>14</sup>C-lactate determinations) or HClO<sub>4</sub> (3%, v/v) (for <sup>3</sup>H<sub>2</sub>O determinations). To quantify <sup>14</sup>C-lactate, cell extracts were neutralized with 1% (w/v) ZnSO<sub>4</sub>, centrifuged at 16,000 x g and 0.5 ml of the supernatant passed through 0.5 x 5 cm Dowex AG 1x8 borate and Dowex AG 1x8 formate tandem columns (BioRad Laboratories)<sup>2,3</sup>. Lactate and glucose elution coefficients were calculated by loading columns with 0.4 ml of a mixture of either 5 mM glucose and 5 mM lactate (standard mixture A), or 2 µCi ml<sup>-1</sup> of [3-<sup>3</sup>H]glucose and 0.5 µCi ml<sup>-1</sup> of [U-<sup>14</sup>C]lactate (standard mixture B). Once loaded with samples or standards, tandem columns were washed with 8 ml of water and separately eluted with 8 ml of 4 M formic acid. Aliquots of 1 ml of the eluates were used to determine spectrophotometrically lactate and glucose concentrations (for standard mixture A) or <sup>3</sup>H and <sup>14</sup>C radioactivity (for eluates of standard mixture B and samples). Using this method, >95% of the radioactivity from glucose and >98% of radioactivity from lactate (from standard mixture B) was recovered from the borate and formate columns at fractions 3-6 and 2-4 of formic acid, respectively. In preliminary experiments, solutions of [3-<sup>3</sup>H]glucose or [U-<sup>14</sup>C]lactate were passed through borate and formate columns in tandem. This was followed by elution of each column separately with formic acid. No <sup>3</sup>H radioactivity was found in any of the ten formic acid fractions collected from the formate columns or <sup>14</sup>C radioactivity in any of the ten formic acid fractions collected from the borate columns. In addition, we found that the <sup>3</sup>H to <sup>14</sup>C ratios delivered by the scintillation counter were 0.007948 (dpm <sup>3</sup>H/dpm <sup>14</sup>C ratio, in channel B) and 0.003650 (dpm <sup>14</sup>C /dpm <sup>3</sup>H ratio, in channel A), indicating almost complete separation of both radioisotopes. These experiments indicate that there was no cross-contamination between [3-<sup>3</sup>H]glucose and [U-<sup>14</sup>C]lactate in the collected fractions. The retention indices (RI) for organic acids are inversely correlated with the pKa using formic acid as eluent in the Dowex AG1x8 formate column<sup>4</sup>. Thus, acidic metabolites of the cellular oxidative metabolism with a lower pKa than lactate (pKa,

3.08), such as pyruvate (pKa, 2.25), aspartate (pKa, 2.1), glutamate (pK, 2.2), or 2-oxoglutarate (pKa, 2.47) have higher RI values than lactate and are retained in the column or eluted after lactate. Other acidic metabolites of the Krebs cycle, such as succinate (pKa, 4.19), malate (pKa, 3.4) and isocitrate (pKa, 3.29), with lower RI values than lactate are eluted with the first few fractions. Thus, the possible contribution of metabolites with pool sizes of the order of those of lactate in the lactate fractions is likely to be insignificant. Citrate (pKa, 3.13) or fumarate (pKa, 3.03), which might co-elute with lactate because of their similar pKa values, could contribute to the lactate fraction only negligibly because of their much lower pool sizes than those to lactate. To quantify  $^3\text{H}_2\text{O}$ , vials were left to equilibrate for 48 h with 1 ml of water, which was used to quantify the  $^3\text{H}$  content by liquid scintillation counting<sup>5,6</sup>. Sufficient counts were collected to achieve a coefficient of variation of the counting rates for  $^{14}\text{C}$  and  $^3\text{H}$  not greater than 2%. Both  $^{14}\text{C}$ -lactate and  $^3\text{H}_2\text{O}$  formation was linear over time for at least 90 min.

**Metabolite determinations.** D-Glucose, D-glucose-6-phosphate (G6P), D-fructose-6-phosphate (F6P) and D-fructose-1,6-bisphosphate (F1,6P<sub>2</sub>) were measured in neutralized perchloric extracts obtained from approximately  $15 \times 10^6$  cells. For D-glucose, the increments in absorbance of the samples were measured at 340 nm in a reaction mixture containing 3.8 mM MgCl<sub>2</sub>, 0.38 mM NADP<sup>+</sup>, 0.38 mM ATP, 1 U ml<sup>-1</sup> of G6PD and 2 U ml<sup>-1</sup> of hexokinase in 38.5 mM Tris-HCl buffer at pH 8 (Ref. <sup>7</sup>). G6P and F6P were measured as the increments in absorbance at 340 nm of the samples in two consecutive coupled reactions, catalyzed by G6PD (0.17 U ml<sup>-1</sup>) and PGI (0.7 U ml<sup>-1</sup>), respectively, in a reaction mixture containing 5 mM MgCl<sub>2</sub> and 0.2 mM NADP<sup>+</sup> in 0.2 M triethanolamine buffer at pH 7.6 (Ref. <sup>8</sup>). For F1,6P<sub>2</sub>, the decrease in absorbance of the samples was measured at 340 nm in a reaction mixture containing 0.017 mM NADH(H<sup>+</sup>), 0.13 U ml<sup>-1</sup> glycerol-3-phosphate dehydrogenase, 0.83 U ml<sup>-1</sup> triosephosphate isomerase and 0.04 U ml<sup>-1</sup> aldolase in a 0.2 M triethanolamine/20 mM EDTA buffer at pH 7.6 (Ref. <sup>9</sup>). For lactate, the increments in absorbance of the samples were measured at 340 nm in a mixture containing 1 mM NAD<sup>+</sup> and 22.5 U ml<sup>-1</sup> lactate dehydrogenase in 0.25 M glycine/0.5 M hydrazine/1 mM EDTA at pH 9.5 (Ref. <sup>10</sup>). For fructose-2,6-bisphosphate (F2,6P<sub>2</sub>) determinations, cell extracts were lysed in 0.1 M NaOH and centrifuged (20,000 g for 20 min). An aliquot of the homogenate was used for protein determination and the remaining sample was heated at 80°C (5 min), centrifuged (20,000 g for 20 min) and the resulting supernatant used for determination of F2,6P<sub>2</sub> concentrations<sup>11</sup>. For glutathione determinations, cell sorted-neurons were treated with 1% (w/v) sulfosalicylic acid and centrifuged at 13,000 x g for 5 min at 4°C. Total (GSx, i.e. the amount of GSH plus 2 times the amount of GSSG) and oxidized glutathione concentrations were measured in the supernatants using the enzymatic method of Tietze<sup>12</sup>. GSSG was quantified after derivatization of GSH in the samples with 2-vinylpyridine. Data were extrapolated to those obtained with GSSG standards (0-5 μM for GSSG; 0-50 μM for GSx). GSH concentrations were calculated as the difference between GSx and 2 x GSSG.

**APC/C ubiquitin ligase activity.** Active APC/C was immunoprecipitated from neurons or astrocytes using monoclonal α-APC3 antibody (Becton Dickinson Biosciences) and immobilized on Dynabeads Protein A (Invitrogen). For ubiquitination, reactions were performed as described<sup>13</sup> at 37 °C in 10 μl of buffer (0.1 M KCl, 2.5 mM MgCl<sub>2</sub>, 2 mM ATP, 7.5 μg ubiquitin, 0.3 mM dithiothreitol, 135 mM MG132, 1 mM ubiquitin aldehyde, 2.5 mM His-UbcH10 and 2.5 μM UbcH5a in 20 mM Tris-HCl, pH 7.5)

containing 2.5 µl of APC/C beads and 1 µl of [<sup>35</sup>S]cyclin B1. Reactions were stopped at the indicated time points with SDS sample buffer, mixtures resolved by SDS-polyacrylamide gel electrophoresis and visualized by phosphorimaging.

*Northern blotting.* Purified (Genelute mammalian total RNA miniprep kit, Sigma) total RNA samples were electrophoresed (15 µg of RNA/line) on a 1% (w/v) agarose-formaldehyde gel. After transfer to a GeneScreen Plus membrane (NEN Life Sci., Boston, MA) and cross-linking by ultraviolet irradiation, membranes were hybridised for 18 h at 65 °C in the presence of random-primed [α-<sup>32</sup>P]dCTP-radiolabelled (Amersham Biosciences, Buckinghamshire, U.K.) cDNA probes for the Pfkfb3 kinase domain and a 0.7 kb cDNA fragment of the rat cyclophilin, used as a loading control. Membranes were then exposed to Kodak XAR-5 film.

*Western Blotting.* Aliquots (100 µg of protein) of neuron lysates (in 2% sodium dodecylsulfate, 2 mM EDTA, 2 mM EGTA, 5 mM Tris, 100 µM phenylmethylsulfonyl fluoride, 50 µg ml<sup>-1</sup> pepstatin, 50 µg ml<sup>-1</sup> amastatin, 50 µg ml<sup>-1</sup> leupeptin, 50 µg ml<sup>-1</sup> bestatin and 50 µg ml<sup>-1</sup> soybean trypsin inhibitor) were centrifuged (14,000 g, 10 min) and electrophoresed in an 8% SDS acrylamide gel. Proteins were transferred electrophoretically to nitrocellulose membranes, which were blocked in 5% (w/v) low-fat milk in 20 mM Tris, 500 mM sodium chloride, 0.1% (w/v) Tween 20 (at pH 7.5) for 1h, and further incubated with antibodies against Pfkfb3 (described in Methods), commercial Pfkfb3 (PFK-2 brain/placental, catalogue number sc-10091; Santa Cruz Biotechnology) PGI (Santa Cruz Biotechnology), Cdh1 (AR38, J. Gannon, Clare Hall Laboratories, Cancer Research UK), Gap43 (Abcam plc, Cambridge, UK), G6PD (J. M. Bautista, Universidad Complutense, Madrid, Spain), Pfkfb2 (C. MacIntosh, University of Dundee, UK), Pfk1/4 (Santa Cruz Biotechnology) or GAPDH (Sigma) overnight at 4 °C. Signal detection was performed with an enhanced chemiluminescence kit (Pierce, Thermo Scientific, Waltham, MA, USA).

*Inmunohistochemistry.* Wistar rats were deeply anaesthetized with a mixture (3:4) of ketamine hydrochloride (Ketolar; Parke-Davis, Barcelona, Spain) and tiacine hydrochloride (Rompún; Bayer, Leverkusen, Germany) using 1 mL of the mixture per kg body weight, and then perfused intra-aortically with 0.9% NaCl, followed by Somogy's fixative without glutaraldehyde (5 mL/g per body weight). After perfusion, brains were dissected out and postfixed with the same fixative for 24 h at 4 °C. Brain blocks were then rinsed for 2 h with 0.1 M phosphate buffer (PB), pH 7.4, and immersed in 30% (w/v) sucrose PB until they sank. After cryoprotection, 30 µm-thick coronal sections were obtained with a freezing-sliding microtome (Leica Frigomobil, Jung SM 2000, Leica, Nussloch, Germany). The sections were collected in 0.05% sodium azide (w/v) in PB at 4 °C. Coronal sections were rinsed in 0.1 M PB, pH 7.4, three times each for 10 minutes, and then incubated sequentially in: (i) 1% sodium borohydride for 20 minutes to remove aldehyde autofluorescence; (ii) 0.2% Triton X-100 and 5% normal donkey serum in PB for 1h at room temperature; (iii) 1:100 goat anti-Pfkfb3 (PFK2 br/pl Santa Cruz Biotechnology sc-10091), 1:5,000 mouse anti-NeuN (No.MAB377, Chemicon international, Temecula, CA, USA), 1:1,000 mouse anti-glial fibrillary acidic protein (GFAP; No.G-3893, Sigma) in 0.2% Triton X-100 and 5% normal donkey serum for 72 h at 4 °C in PB; (iv) 0.1 µg/mL DAPI in PB for 10 minutes at room temperature and; (v) 1:400 Cy2-conjugated donkey anti-goat, 1:400 Cy3-conjugated donkey anti-mouse (all the secondary antibodies are from Jackson Immunoresearch, Pennsylvania, U.S.A.) in PB for 2 h at room temperature. Between

each step, the sections were carefully rinsed three times each for 10 minutes in PB. After rinsing, sections were mounted with an antifading medium. Sections were examined using both a microscope (Provis AX70; Olympus, Tokyo, Japan) equipped with epifluorescence and appropriated filters sets, and a confocal microscope (TCS SP2; Leica, Mannheim, Germany).

*Accession numbers.* Pfkfb1 (NM\_012621), Pfkfb2 (NM\_080477), Pfkfb3 (NM\_057135), Pfkfb4 (NM\_019333), PGI (NM\_207192), Cdh1 (NM\_016263), and cyclin B1 (AY338491).

## References

1. Watanabe, F., Sakai, A. & Furuya, E. Novel isoforms of rat brain fructose 6-phosphate 2-kinase/fructose 2,6-bisphosphatase are generated by tissue-specific alternative splicing. *J Neurochem* **69**, 1-9 (1997).
2. Hammerstedt, R. H. The use of Dowex-1-borate to separate 3HOH from 2-3H-glucose. *Anal Biochem* **56**, 292-3 (1973).
3. Huang, M. & Veech, R. L. The quantitative determination of the in vivo dephosphorylation of glucose 6-phosphate in rat brain. *J Biol Chem* **257**, 11358-63 (1982).
4. Thauer, R. K., Rupprecht, E. & Jungermann, K. Separation of 14C-formate from CO<sub>2</sub> fixation metabolites by isoionic-exchange chromatography. *Anal Biochem* **38**, 461-8 (1970).
5. Katz, J., Rognstad, R. & Kemp, R. G. Isotope Discrimination Effects in the Metabolism of Tritiated Glucose. *J Biol Chem* **240**, PC1484-6 (1965).
6. Hughes, S. D., Quaade, C., Johnson, J. H., Ferber, S. & Newgard, C. B. Transfection of AtT-20ins cells with GLUT-2 but not GLUT-1 confers glucose-stimulated insulin secretion. Relationship to glucose metabolism. *J Biol Chem* **268**, 15205-12 (1993).
7. Bergmeyer, H. U., Bernt, E., Schmidt, F. & Stork, H. in *Methods of Enzymatic Analysis* (ed. Bergmeyer, H. U.) 1196-1201 (Verlag Chemie GmbH, Weinheim, 1974).
8. Michal, G. in *Methods of Enzymatic Analysis* (eds. Bergmeyer, J. & Graßl, M.) 191-198 (Verlag Chemie, Weinheim, Deerfield Beach (FL), Basel, 1985).
9. Michal, G. in *Methods of Enzymatic Analysis* (eds. Bergmeyer, J. & Graßl, M.) 342-350 (Verlag Chemie, Weinheim, Deerfield Beach (FL), Basel, 1985).
10. Gutmann, I. & Wahlefeld, A. W. in *Methods of Enzymatic Analysis* (ed. Bergmeyer, H. U.) 1464-1468 (Verlag Chemie GmbH, Weinheim, 1974).
11. Van Schaftingen, E., Lederer, B., Bartrons, R. & Hers, H. G. A kinetic study of pyrophosphate: fructose-6-phosphate phosphotransferase from potato tubers. Application to a microassay of fructose 2,6-bisphosphate. *Eur J Biochem* **129**, 191-195 (1982).
12. Tietze, F. Enzyme method for quantitative determination of nanogram amounts of total and oxidized glutathione: application to mammalian blood and other tissues. *Anal. Biochem.* **27**, 502-522 (1969).
13. Kimata, Y. et al. A mutual inhibition between APC/C and its substrate Mes1 required for meiotic progression in fission yeast. *Dev Cell* **14**, 446-54 (2008).